



High-yield decomposition of surface EMG signals

S. Hamid Nawab^{b,c,d}, Shey-Sheen Chang^a, Carlo J. De Luca^{a,b,c,d,e,*}

^a Delsys Inc., Boston, MA 02215, USA

^b Department of Electrical and Computer Engineering, Boston University, Boston, MA 02215, USA

^c NeuroMuscular Research Center, Boston University, Boston, MA 02215, USA

^d Department of Biomedical Engineering, Boston University, Boston, MA 02215, USA

^e Department of Neurology, Boston University, Boston, MA 02215, USA

ARTICLE INFO

Article history:

Accepted 19 November 2009

Available online 28 April 2010

Keywords:

Decomposition
Surface EMG
Motor units
Action potentials
Firings
Firing rate

ABSTRACT

Objective: Automatic decomposition of surface electromyographic (sEMG) signals into their constituent motor unit action potential trains (MUAPTs).

Methods: A small five-pin sensor provides four channels of sEMG signals that are in turn processed by an enhanced artificial intelligence algorithm evolved from a previous proof-of-principle. We tested the technology on sEMG signals from five muscles contracting isometrically at force levels ranging up to 100% of their maximal level, including those that were covered with more than 1.5 cm of adipose tissue. Decomposition accuracy was measured by a new method wherein a signal is first decomposed and then reconstructed and the accuracy is measured by comparison. Results were confirmed by the more established two-source method.

Results: The number of MUAPTs decomposed varied among muscles and force levels and mostly ranged from 20 to 30, and occasionally up to 40. The accuracy of all the firings of the MUAPTs was on average 92.5%, at times reaching 97%.

Conclusions: Reported technology can reliably perform high-yield decomposition of sEMG signals for isometric contractions up to maximal force levels.

Significance: The small sensor size and the high yield and accuracy of the decomposition should render this technology useful for motor control studies and clinical investigations.

© 2010 International Federation of Clinical Neurophysiology. Published by Elsevier Ireland Ltd. All rights reserved.

1. Introduction

Researchers in the field of motor control and clinicians managing patients with motor disorders wanting to observe the firing behavior of motor units have been limited to using cumbersome technology having unquantifiable accuracy. In this study, we report a system that estimates the firing patterns of a significant fraction of the active motor units in a muscle during a contraction. The system is a maturation of the proof-of-principle reported by De Luca et al. (2006). The technology, an advancement of the original Precision Decomposition approach of LeFever and De Luca (1982), decomposes the surface electromyographic (sEMG) signal that is detected non-invasively from the surface of the skin. These sEMG signals have been successfully decomposed for contraction forces ranging from minimal to 100% of Maximum Voluntary Contraction (MVC) levels.

The use of the sEMG signal offers several advantages over the indwelling EMG signals acquired with needle or wire sensors. There is no need for clinical preparations such as sterilization

of sensor or placement site; there is no risk of infection or disease transmission; there is no potential for muscle tissue damage; sensitive or dangerous areas such as eyelids, lips, and tongue need not be excluded. Another advantage is that the sEMG signal contains contributions from a greater number of motor units, thus providing a richer expression of the motor unit behavior during a contraction.

Decomposition of sEMG signals into time-frequency components (Englehart et al., 1999), wavelet components (Englehart et al., 2001) and degrees-of-freedom force functions (Jiang et al., 2009) has been very successful for applications in prosthesis control. However, sEMG signal decomposition into motor unit action potential trains (MUAPTs) has till now by and large proved to be a difficult problem (Merletti and Parker, 2004), although different methods have been proposed and investigated by us (De Luca et al., 2006) and others, including Zhou et al. (2006) and Holobar and Zazula (2007). Such efforts have been mainly inspired by the high degree of success (LeFever and De Luca, 1982; Stashuk, 2001; McGill et al., 2005; Nawab et al., 2008; Erim and Lin, 2008) that has been achieved in the decomposition of indwelling EMG signals, even though they are generally less challenging to decompose than sEMG signals.

* Corresponding author at: Delsys, Inc., 650 Beacon Street, 6th Floor, Boston MA 02215, USA. Tel.: +1 617 353 9756.

E-mail address: cjd@bu.edu (C.J. De Luca).

2. Methods

The system of this report consists of a 5-pin surface sensor, a signal acquisition system, and a signal decomposition algorithm. In this section, we describe each of these components as well as the rationale for the experiments that were conducted to evaluate the performance of the system. Note that these experiments were performed for the sole purpose of testing the technology and not for performing comprehensive physiological investigations.

2.1. The sEMG sensor

The 5-pin surface sensor of this report is shown in Fig. 1A attached above the FDI muscle. The sensor consists of five cylindrical pins (0.5 mm diameter each) with blunted ends that protrude from the housing so that when pressed against the skin they make a surface indentation, but do not puncture the skin. As illustrated in Fig. 1B, the pins are placed at the center and at the corners of a 5 × 5-mm square. Pair wise subtraction of voltages at the five detection surfaces is used to derive multi-channel sEMG signals. The subtraction ensures that common-mode signals (such as those due to external electrical sources) undergo a high degree of cancellation. As discussed in LeFever and De Luca (1982), the utilization of multi-channel EMG signals (typically 3 or 4 channels) improves the ability of decomposition systems to discriminate the motor

unit action potential (MUAP) of one motor unit from that of another.

2.2. EMG signal acquisition

The sEMG sensor and a reference electrode are connected to four channels of a Bagnoli sEMG system from Delsys Inc. We typically select four channels which have the greatest signal to noise ratio. The analog sEMG channels are high-pass filtered with a cutoff frequency of 20 Hz (24 dB/octave roll-off) and lowpass filtered with a cutoff frequency of 1750 Hz (24 dB/octave roll-off). Each channel is then over-sampled at 20 KHz (to avoid introducing significant phase skew across channels) and the resulting digital data are stored on a computer for decomposition processing as well as for post-decomposition analysis of action potential morphology. When the decomposition is initiated, the digital sEMG signals are digitally filtered with a high-pass filter having a cutoff frequency of 50 Hz (24 dB/octave roll-off). This latter filtering stage removes the long tails of the action potentials, thus reducing the incidence of superposition between the action potentials and making the decomposition task relatively less challenging.

2.3. Data collection

Eight neurologically healthy subjects (4 males and 4 females) having age ranging from 21 to 41 years (26.9 ± 7.8 yrs) volunteered for the data collection experiments. All read, understood and signed an Informed Consent form provided by the Institutional Review Board of Boston University. Measurements were made on the First Dorsal Interosseous (FDI) muscle, the Vastus Lateralis (VL) muscle, the Tibialis Anterior (TA) muscle, the Biceps Brachialis (BB) muscle, and the Biceps Femoris (BF) muscle. These muscles were chosen because they are different in sizes, have different recruitment and firing rate strategies (De Luca et al., 1982,1996; Adam and De Luca, 2005), and are covered by different amount of adipose tissue. Thus, the sEMG signal from these muscles would provide different challenges to the system.

The subjects were requested to perform constant-force isometric contractions by tracking a trapezoidal force paradigm presented on a screen. The trapezoid increased from zero to the target force in 2–5 s, remained constant for 5–15 s, and decreased to zero in 2–5 s. The constant-force level varied from 20% to 100% MVC. The force level was measured by placing the appropriate limb in an apparatus that restrained the movement of the limb and was instrumented with a high-stiffness force gauge (model MB-250; Interface, Scottsdale, AZ). The MVC was taken as the maximal value of three sequential efforts at generating the maximal force level. The subjects were asked to contract as forcefully as possible and hold the contraction for 2–3 s. Each attempt was followed with a rest period of 5 min.

2.4. Signal decomposition algorithm

The signal decomposition algorithm begins by extracting action potential “templates” of as many MUAPTs as practically possible from the input sEMG signal, and then it searches for signal regions where the extracted templates are in superposition with each other or with unidentified action potentials. The algorithm takes both constructive and destructive interference effects¹ into account when analyzing such superpositions and it requires that the unidentified action potentials account for less than 25% of the signal energy at the firing locations of the decomposed MUAPTs. The only assump-

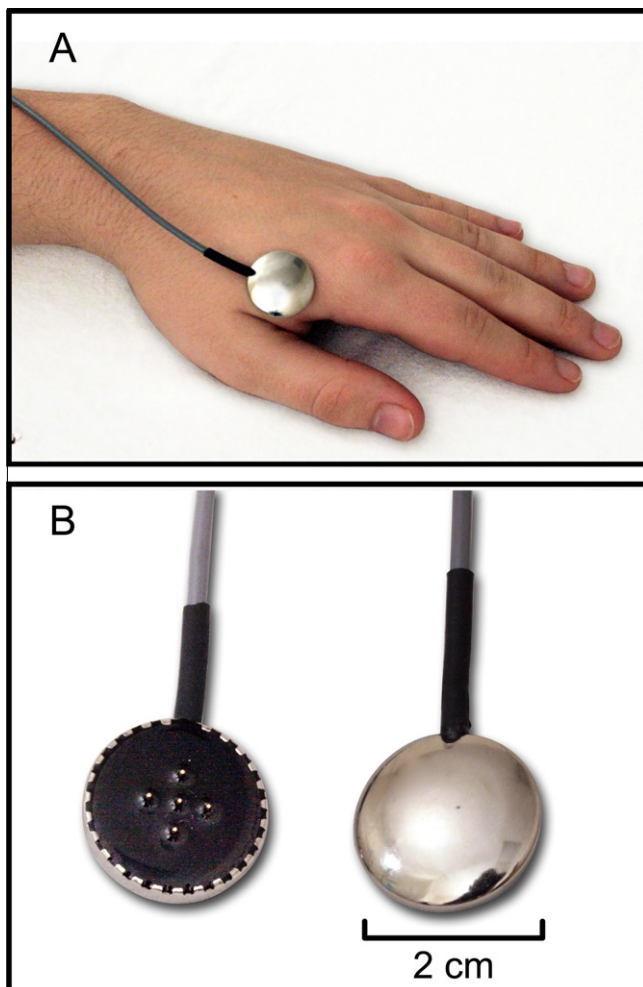


Fig. 1. (A) The five-pin surface EMG sensor attached above the First Dorsal Interosseous muscle in the hand. (B) Top and bottom views of the sensor. The four pins on the corner of a square are spaced 3.6 mm apart.

¹ The extreme of completely destructive interference is not considered as a possibility by the algorithm because it is essentially impossible to detect. It is, however, also a rare (although not impossible) occurrence in the sEMG signal.

tion made about inter-pulse intervals during this process is that they be less than 0.35 s.

The algorithm is designed so as to typically decompose 20–30 MUAPTs per contraction. In steady state, such constituents collectively contribute on the order of 300–600 MUAP firings per second. After high-pass filtering to eliminate non-MUAP signal sources and some low-frequency components of the MUAPs, each MUAP has a main lobe and significant side lobes that together are on the order of 5–10 ms long. It follows that in steady state each decomposed MUAP instance typically overlaps to some degree with at least 3–6 other decomposed MUAP instances, and at times more. Also, there is additional superposition with MUAP firings of the lower-amplitude non-decomposed MUAP constituents. Because of such a high degree of MUAP superposition and because the MUAP shape of each MUAPT always has temporal variability, the decomposition task is very challenging.

Our decomposition algorithm was designed utilizing well-established technology from the knowledge-based systems sub-field (Leondes, 2000) of artificial intelligence. Knowledge based algorithms have been widely used in physiological signal applications such as ECG interpretation (Kundu et al., 2000) and EEG seizure detection (Aarabi et al., 2007) and in non-physiological signal applications such as remote sensing (Bárdossy and Samaniego-Eguiguren, 2002) and radar signal classification (Gini and Rangaswamy, 2008). They are generally designed to operate in real life situations and thus are characterized by their use of a knowledge base of empirically sustainable “rules” (Ligeza, 2006) and “cases” (Leake, 2000) that can continually and conveniently be added to, removed, or modified for improved performance. The updating of rules and cases is akin to the updating of the weights of a neural network in response to experience with new data. However, in both cases, the updating takes place in the context of an existing internal structure. The rules, cases, or weights may change as the system encounters new types of situations, but this internal structure remains invariant.

The reported system’s invariant internal structure builds upon the Precision Decomposition (PD) approach originated by Lefever and De Luca (1982). We have previously utilized the PD approach in conjunction with the Integrated Processing and Understanding (IPUS) concept (Lesser et al., 1995) from artificial intelligence to develop a decomposition algorithm for indwelling EMG signals (Nawab et al., 2002, 2004, and Nawab et al., 2006). The IPUS framework basically allows rules to be conveniently encoded (see Wino-

grad and Nawab (1995) for details) in support of the mathematical structure of an algorithm in order to permit run-time modification of its behavior in response to different conditions found in the input signal. For example, in the context of the PD approach, the IPUS rules help to decide on a signal-by-signal basis what amplitude threshold to use in detecting action potentials so that their shapes can be resolved sufficiently for distinguishing them from action potentials of other MUAPTs. A variant of the PD-IPUS algorithm was used in a proof-of-principle demonstration by De Luca et al. (2006) (with improvements reported by Nawab et al. (2008), Chang et al. (2008) and Nawab et al. (2009)) that an artificial intelligence approach can be used to obtain the MUAPT constituents of the complex sEMG signal. While the PD-IPUS algorithm of De Luca et al. (2006) is typically able to extract templates for 20–30 MUAPTs from the sEMG signal, it is unable to adequately resolve their complex superpositions except in the case of 4–8 MUAPTs of highest amplitude. The signal decomposition algorithm of this report represents the result of introducing new mechanisms that help to resolve complex superpositions for a larger number of the MUAPTs identified by the original PD-IPUS algorithm.

As indicated in the block diagram of Fig. 2, the sEMG signal decomposition algorithm of this report begins with an initial PD-IPUS stage to identify as many templates for the various MUAP shapes as possible. It then follows with an “iterative generate and test” stage (PD-IGAT) of artificial intelligence to identify the templates whose presence is objectively indicated in any of the complex superpositions within the sEMG signal. More details of the PD-IPUS and PD-IGAT stages are described next.

2.5. PD-IPUS stage

The PD-IPUS stage of the new algorithm is, for the most part, the same as the algorithm reported by De Luca et al. (2006). It is a combination of three basic processes: MUAP template creation, MUAP template matching, and MUAP template updating. The creation of MUAP templates involves the extraction of signal shapes in the vicinity of data peaks in the sEMG signal. The matching of MUAP templates against the remaining sEMG signal takes place through a Maximum A-posteriori Probability classifier. Updating of MUAP templates takes place through a recursive weighting process (Nawab et al., 2002) whenever the matching procedure detects a new instance of a previously detected MUAP.

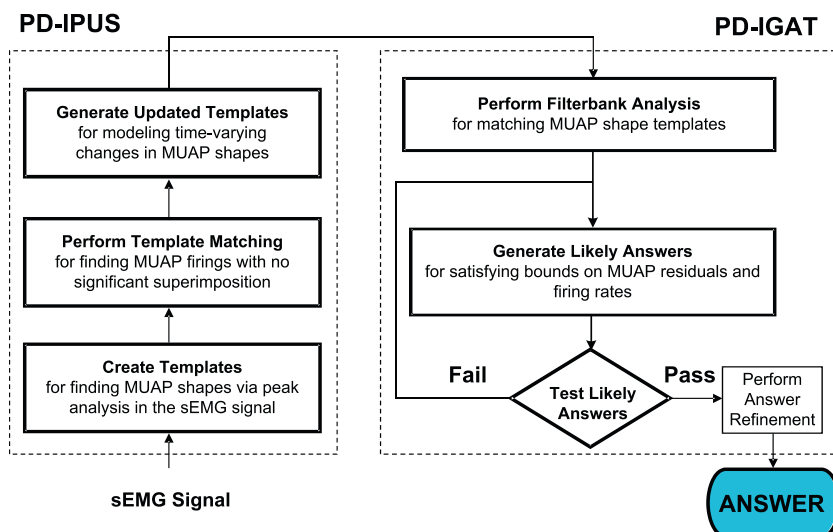


Fig. 2. Block diagram of the sEMG signal decomposition algorithm. The PD-IPUS stage creates, matches, and updates motor unit action potential (MUAP) templates. The PD-IGAT stage performs MUAPT discrimination at the output of a shape-matching procedure applied to the sEMG signal.

2.6. IGAT stage

The PD-IGAT stage begins by applying a template-matching procedure (Chang et al., 2008) to the sEMG signal for identifying signal locations where the shape of the sEMG signal and the shape of a MUAPT template from the PD-IPUS stage exhibit a correlation above an adaptive threshold of at least 20% with each other². The PD-IGAT stage then performs iterative MUAPT discrimination analysis (Nawab et al., 2009, Chang et al., 2008) at each of those signal locations to determine which, if any, of the multiple matching templates have actually contributed there. A brute force solution would be to try all possible combinations of the matching templates so as to determine which combination models the sEMG signal in that vicinity with the greatest accuracy. Since each location is typically associated with the templates of on the order of five different MUAPTs, such a brute force approach becomes computationally prohibitive. Instead, we utilize a process by which template combinations of greater likelihood are considered first and the search is stopped if an acceptable³ level of signal modeling accuracy is attained by 2 of the combinations or if the 10 most likely combinations have been considered and fewer than 2 of them have been deemed acceptable. The likelihood of a template combination at a particular signal location is determined on the basis of (1) the degree to which each of the combination's constituent templates matches the signal shape in the vicinity of that location and (2) the degree to which the location is consistent with a locally estimated firing rate for the corresponding MUAPT. More formally, the process of likelihood assignment for the various combinations is carried out by invoking a statistical utility maximization procedure as described by Nawab et al. (2004). Once the template combinations (and their acceptable competitors at some of the locations) have been selected for the entire sEMG signal, the resulting MUAPTs are required to meet the following criteria:

- The mean energy of the residual signal (the difference between the original signal and all the identified MUAPTs) at the firing locations of any MUAPT must be a relatively small fraction ($\alpha \leq 0.25$) of the mean energy in all the MUAPT constituents at those locations.
- The mean inter-pulse interval of any MUAPT during its active periods must not be greater than τ seconds. We use $\tau \geq 0.35$ s in our current implementation of the algorithm. It should be noted that in the current implementation of the algorithm if a MUAPT does not have any firings for at least half a second, it is considered to be inactive until it next begins firing again with an inter-pulse interval of at least 0.35 s.

If competing answers for any MUAPT satisfy both of the above test criteria, the answer with the smallest coefficient of variation for its inter-pulse intervals is selected.⁴

The final “answer refinement” phase of the PD-IGAT stage is designed to adjust or re-position the firing locations of the selected MUAPT answers by taking greater account of their mutual superposition effects. A “peel off and match” strategy is used in which the action potential templates of the answer MUAPTs are consid-

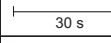
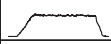
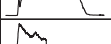
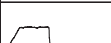
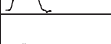
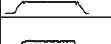
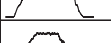
ered in order of MUAP size, from largest to smallest. When re-positioning a particular firing time of a given MUAPT, this strategy subtracts (“peels off”) the action potential templates of all the larger MUAPTs from their previously re-positioned locations in the sEMG signal and then cross-correlates (“matches”) the result with the given MUAPT's action potential template. The firing time of the given MUAPT is then re-positioned to the location of the nearest peak in the resulting cross-correlation function.

3. Results

The sEMG signal decomposition algorithm was systematically tested on a database of 22 sEMG signals acquired from five muscles contracting at levels ranging from 20% to 100% MVC. A detailed assessment of algorithm performance on our signal database is summarized in Table 1. For each numbered element of the data-

Table 1

Summary of results from the application of the reported sEMG decomposition algorithm to a database of 22 real 4-channel sEMG signals. The number of MUAPTs decomposed by the algorithm on this database ranges from 16 to 40. The number of MUAPs found per second ranges from 231 to 742, and processing time per MU per second ranges from 2.3 to 4.6 s. Muscle abbreviations used: FDI, First Dorsal Interosseus, TA, Tibialis Anterior, VL, Vastus Lateralis, BB, Biceps Brachialis and BF, Biceps emoris.

	Muscle	Contraction Time	%MVC	Force Profile 	# MUs found	# MUAPs found per sec	Processing Time (per MU per sec)
1	FDI	25 s	50		30	632	4.2 s
2		25 s	50		24	436	3.4 s
3		20 s	70		21	358	3.2 s
4		25 s	30		24	504	3.9 s
5		25 s	50		28	629	3.8 s
6		22 s	70		24	511	3.1 s
7		20 s	80		24	566	3.6 s
8		15 s	100		19	438	3.8 s
9	VL	20 s	50		31	418	3.9 s
10		25 s	50		16	198	4.6 s
11		22 s	70		24	312	2.5 s
12		20 s	80		33	558	3.6 s
13		10 s	100		18	286	2.4 s
14	TA	15 s	20		16	231	3.9 s
15		14 s	50		22	362	3.6 s
16		20 s	80		28	447	3.7 s
17		15 s	100		21	325	4.1 s
18	BB	24 s	25		28	490	3.7 s
19		27 s	50		21	307	4.1 s
20		25 s	75		39	547	2.3 s
21	BF	15 s	40		30	434	4.2 s
22		15 s	40		40	742	3.5 s

² Signal to template correlations as low as 20% are deemed to be possible matches because the sEMG signal is expected to contain excessive amounts of inter-MUAPT superposition.

³ The modeling accuracy of a template combination at a signal location is considered acceptable if subtracting the template combination from the signal location reduces the signal energy at that location by an adaptive threshold that is at least 50% of the net energy in the template combination.

⁴ The rationale for this phase of PD-IGAT is that random placements of false positives and/or false negatives amongst the firings of a MUAPT always tend to increase MUAPT inter-pulse irregularity. The true firings would therefore be expected to cause a minimum in inter-pulse irregularity.

base, Table 1 lists various attributes of the corresponding muscle contraction (muscle type, peak force level, duration, and force profile generated). It also provides various metrics on how well our algorithm performed in decomposing the signal. The algorithm is found to produce 16–40 MUAPTs per contraction while detecting (at peak force) 200–750 action potentials per second. Its processing speed on a Personal Computer was found to be on the order of 3 s for each second of any decomposed MUAPT.

Let us now examine more detailed results of sEMG signal decomposition obtained on the experimental database of 20 sEMG signals.

3.1. MUAPT inter-pulse intervals

The inter-pulse intervals of 30 MUAPTs obtained by decomposing an sEMG signal (signal # 1 of Table 1) from a 50% MVC of the FDI muscle are shown in Fig. 3. This type of a plot is referred to as a “dot” plot in which each MUAPT’s inter-pulse intervals are represented by a series of dots. The horizontal and vertical coordinates of each dot, respectively, represent a specific firing time and the time elapsed since the immediately preceding firing of the same motor unit. Superimposed on the dot plot is a solid line that represents the force profile generated during the muscle contraction. The vertical axis on the left represents the recruitment order of MUAPT constituents while the vertical axis on the right represents force level as a percentage of MVC. The behavior of the inter-pulse intervals is consistent with that observed in data obtained from our previous decomposition methods (De Luca et al., 1982, 1996; De Luca and Erim, 2002) decomposition procedures of other researchers (McGill et al., 2005; Stashuk, 1999), and that observed by visual inspection (Tanji and Kato, 1973; Person, 1974). For example, it can be seen from Fig. 3 that earlier recruited motor units typically have a smaller mean inter-pulse interval than later recruited motor units, corresponding to the increasingly lower firing rates of later

recruited motor units. Later recruited motor units tend to have greater variance in inter-pulse interval than earlier recruited motor units, as reported by Tracy et al. (2005) and Contessa et al. (2009). Also, the dots (inter-pulse intervals) of each MUAPT decrease in height as the force increases and fluctuate about an average value when the force of the trapezoidal profile is constant. The recruitment order of motor units is highly correlated with the de-recruitment order (De Luca et al., 1982; Person, 1974).

3.2. Time sequence of MUAPT firing times

The firing times of each MUAPT are commonly plotted in the form of vertical “bars.” Such a bar plot is shown in Fig. 4 for 28 MUAPTs of a 0.5 s interval of an sEMG signal (signal #5 in Table 1) from the FDI Muscle at 50% MVC. The entire waveform for one channel of the contraction is shown at the top of Fig. 4 along with a time-expanded plot of the highlighted 0.5 s interval. The left vertical axis on the bar plot represents the recruitment order of MUAPTs and the right vertical axis represents force level as a percentage of MVC. Inspection of the bar plot in Fig. 4 confirms the now generally accepted observation that later recruited motor units tend to have greater inter-pulse intervals, corresponding to lower mean firing rates. Finally, in Fig. 5, we show a complete bar plot along with a corresponding force profile for a sEMG signal (signal # 13 in Table 1) acquired at 100% MVC from the VL muscle. The initial recruitment period of such contractions is extremely short (less than 1 sec in this case) because the subject is attempting to achieve 100% MVC. This makes it difficult for the algorithm to precisely locate the recruitment times, particularly for the later recruited motor units. In this particular instance, the recruitment times appear to conform to what one would expect for the superimposed force profile in Fig. 5, including the second recruitment of motor unit 15.

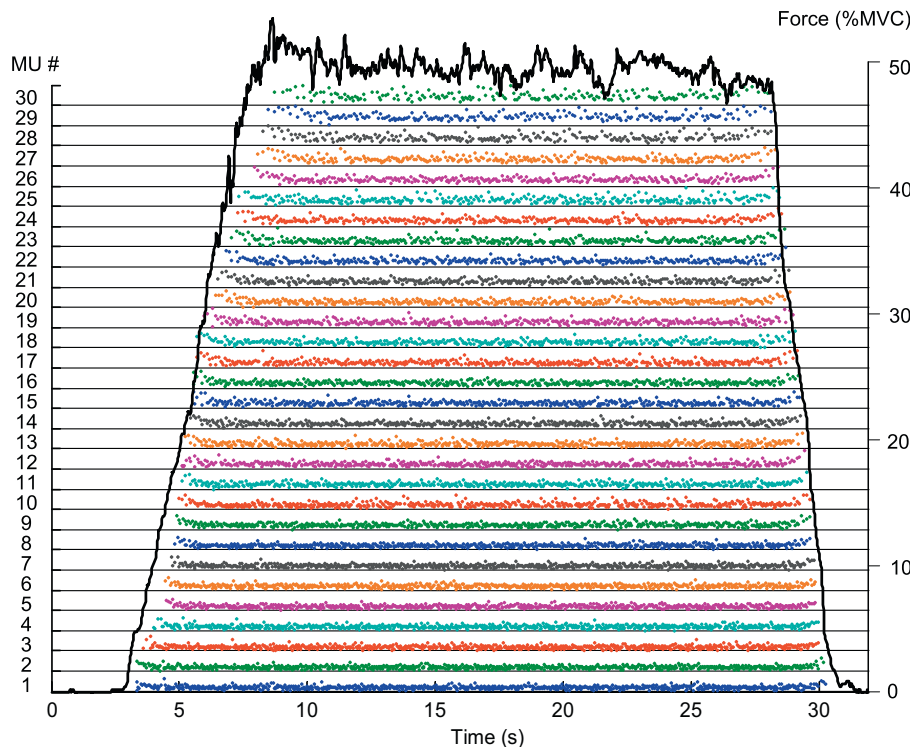


Fig. 3. Dot plots of inter-pulse intervals of 30 MUAPTs obtained by decomposing signal # 1 of Table 1. The Inter-pulse-interval is plotted vertically. The vertical limit on each dot height is 200 ms. The sEMG signal was collected during a 50% MVC of the FDI muscle. The numbers left of the vertical axis indicate the number and recruitment order of the motor units. Right vertical axis indicates %MVC level of force profile superimposed on the dot plot.

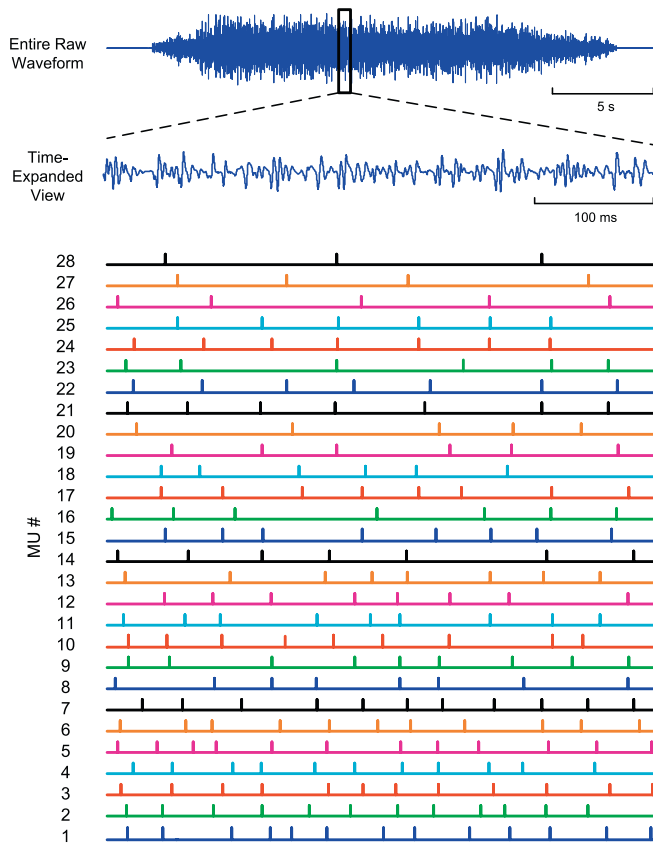


Fig. 4. The top trace represents one channel of the sEMG signal taken from signal #5 in Table 1. It was obtained from a 50% MVC of the First Dorsal Interosseous muscle. The second is an expanded segment (0.5 s) of the raw signal. The bar raster contains the firing times of 28 motor units, numbered according to their recruitment order.

3.3. Residual signal

Shown in Fig. 6 is the entire waveform of a single channel of the sEMG signal (signal #2 in Table 1) acquired from the FDI muscle of a subject performing an isometric contraction at 50% MVC. The corresponding residual signal for the decomposition is shown directly below the sEMG signal of Fig. 6. This residual signal was obtained by removing peaks in the signal data that match the corresponding templates of the 21 identified MUAPTs. The residual indicates that while our signal decomposition algorithm has accounted for a significant number of data peaks in the signal, there are still many data peaks (mostly of smaller amplitudes) left unexplained by the algorithm. This is to be expected since the algorithm is decomposing only 21 motor units while there are considerably more motor units active in the FDI muscle during a 50% MVC contraction. The remaining MUAPTs are not decomposed because of their relatively lower amplitudes at the sEMG sensor location or because the PD-IPUS stage is not able to detect a sufficient number of uncontaminated instances of their action potentials.

3.4. The MUAP shapes

In Fig. 7, we show the 39 MUAP shapes estimated for a 0.5 s interval of a sEMG signal (signal #20 in Table 1) obtained from another muscle, the BB muscle, at 75% MVC. Note that the amplitude of the MUAPs tends to increase with increasing motor unit number, which correspond to the order of recruitment. The amplitude of the

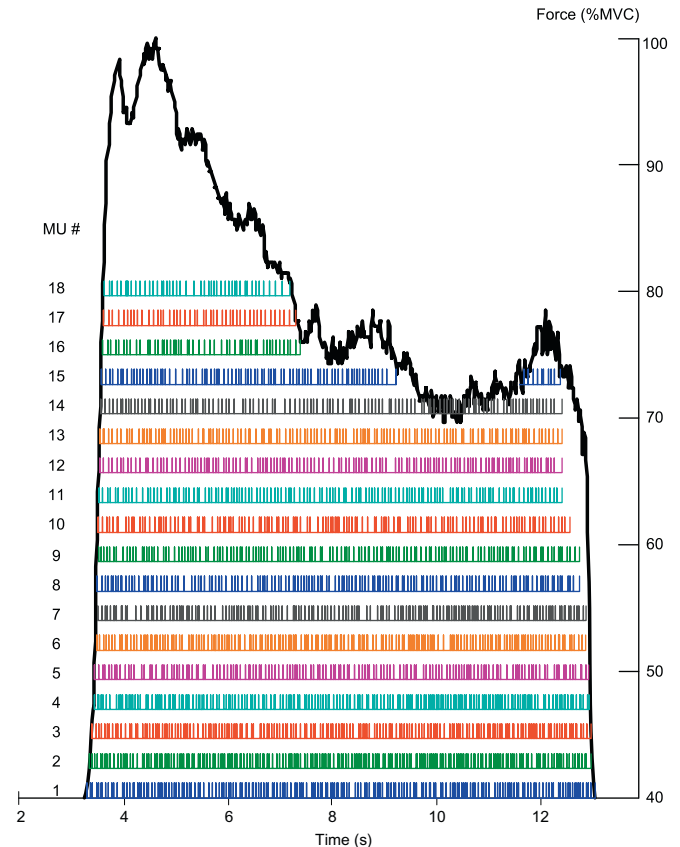


Fig. 5. Bar plot with force profile for signal #13 in Table 1 obtained from a 100% MVC of the Vastus Lateralis muscle. The muscle was covered with 14 mm of adipose tissue. Note that the last detected motor unit was recruited at approximately 80% MVC. Also, motor unit 15 is re-recruited when the force rises up for a second time.

MUAP is indicative of a greater number of muscle fibers contributing to the action potential, or greater action potentials from muscle fibers of greater diameter, or both. The imperfect sequential increase in the amplitude of the MUAP is likely due to the uneven distance between the fibers of some motor units and the sensor. Nonetheless, the display is consistent with the Henneman size principle.

3.5. Accuracy evaluation

Any attempt at decomposing a signal such as the sEMG signal that consists of superimposed pulses (action potentials) of unknown number, of different and varying shapes belonging to a limited, but unknown, set of MUAPTs must provide a proof for the degree of accuracy of the attained identifications. Such a proof cannot be obtained by examining the decomposition performance on mathematically simulated signals of the type used by Holobar et al. (2009) because such signals inevitably lack the realism of actual EMG signals (Mambrito and De Luca, 1984). It is clearly evident that the MUAPs present in the sEMG signal contain inflections that are not easily included in mathematically generated signals, and which vary amongst MUAPs and in different contractions. Another approach, earlier suggested by us (De Luca et al., 2006), compares the instances of firings of the same MUAP train decomposed from a surface EMG signal and an indwelling EMG signal, although improving on the previous approach, is also insufficient. That is so because the degree of agreement between two imperfect decompositions does not offer sufficient proof about the degree of accuracy of either one.

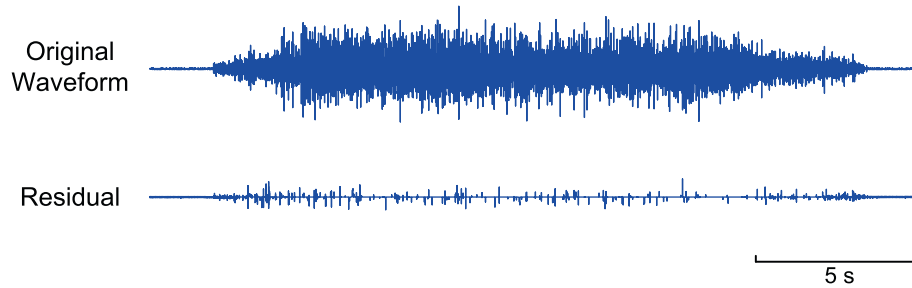


Fig. 6. Plot of entire waveform of a single channel of signal #2 in Table 1 from 50% MVC of the FDI muscle. Plotted directly below is the residual signal from decomposing the top waveform into 24 MUAPTs.

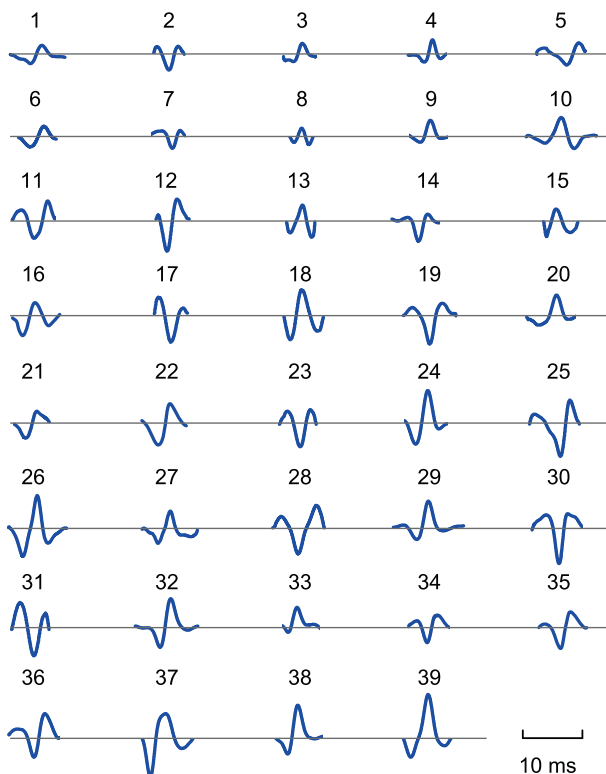


Fig. 7. Plots of 39 MUAP shapes estimated for a 0.5 s interval of signal # 20 in Table 1 obtained from a 75% MVC of the Biceps Brachii muscle. The MUAPs are numbered in their order of recruitment.

A substantial proof of the level of accuracy must answer the following two fundamental questions that govern the quality of the decomposition algorithms:

- (1) To what degree does the algorithm succeed in identifying, for each decomposed motor unit, instances of its action potential shape that are uncontaminated by superposition with other action potentials?
- (2) To what degree does the algorithm succeed in resolving complex superpositions of the action potentials from the different motor units?

We have devised and carried out a method for answering these questions in the context of the sEMG signal decomposition algorithm described in this report. We begin in the context of the first question by observing that our algorithm identifies uncontaminated action potential shapes by utilizing the Maximum A-posteriori Probability (MAP) classifier of Lefever and De Luca

(1982). This classifier was originally designed to perform the same task on indwelling EMG signals. For it to work on the sEMG signal, each decomposable motor unit should have a minimum number of firings (say N) whose action potentials are uncontaminated (via superposition) by action potentials of other motor units. Furthermore, the number N should be large enough to make it essentially impossible for two (or more) decomposable motor units to have N separate instances of simultaneous firings without additional contamination; this ensures that such simultaneous firings are not mistaken for uncontaminated firings of a single motor unit. We have used the value $N = 10$ for 30 s contractions (and proportionately larger values for longer contractions) in our algorithm as a conservative choice⁵ for avoiding the possibility of such confusion. When applied to the 22 signals of our experimental sEMG database, our decomposition algorithm identified an average of 19 uncontaminated action potentials in less than 30 s of activity of each decomposed motor unit. Since the MAP classifier permits the action potential shapes to vary slowly over time (LeFever and De Luca, 1982), it should also be noted that the decomposition algorithm of this report utilizes the nearest uncontaminated action potential of a MUAPT as the template to be used in resolving a complex superposition in which that MUAPT may be involved.

We now proceed to the second question about the degree to which our algorithm can accurately resolve complex superpositions of action potentials from different motor units in the remainder of the sEMG signal. For this purpose, we have devised a reconstruct-and-test procedure and applied it to each of the 22 signals in our experimental sEMG database. The procedure is designed to: (1) “reconstruct” each signal of the database from its uncontaminated action potential shapes, algorithm-identified firing times, and additive Gaussian noise, and (2) to test the decomposition algorithm’s accuracy in resolving complex superpositions by applying it to those reconstructed signals.

Detailed steps of the reconstruct-and-test procedure are illustrated in Fig. 8. Step 1 is to decompose a database sEMG signal $s(n)$. Step 2 is to sum the decomposed MUAPT constituents of $s(n)$ to obtain a synthesized signal $g(n)$. Note that this signal, $g(n)$, just like the original signal $s(n)$, has significant time intervals over which the density of decomposable action potentials reaches several hundreds per second and both signals have similarly-shaped action potentials for their decomposable motor units. To account for the indecomposable motor units (residual signal) of $s(n)$, in Step 3 we obtain a noisy reconstructed signal $y(n)$ by adding white Gaussian

⁵ Rationale: Because it is relatively rare for different motor units to fire simultaneously (De Luca and Adam, 1999), less than 10% of the firings of any motor unit, say A, would be expected to be simultaneous with firings of any other single motor unit. Because the sEMG signal is crowded, less than 10% of the simultaneous firings would be spared contamination by other motor units. Thus, less than 1% of motor unit A’s firings would be simultaneous with one other motor unit and have no additional contamination. That corresponds to less than 6 firings even if motor unit A has a total of 600 firings in 30 s. Thus $N = 10$ is a conservative choice.

noise to $g(n)$. The variance of the added noise is set to the measured variance of the residual signal, $r[n] = s[n] - g[n]$. Step 4 of the procedure uses our sEMG signal decomposition algorithm to decompose $y(n)$. Since the decomposed MUAPT constituents of $s(n)$ are the actual MUAPT constituents of $y(n)$, we are able to identify the false positives and false negatives in the decomposition of $y(n)$ ⁶. The decomposition accuracy obtained this way for the synthesized signals is arguably reflective of the degree to which superpositions are correctly resolved in the corresponding database signals.

The histogram in Fig. 9(A) shows the accuracy levels achieved by the 561 MUAPTs of the 22 reconstructed signals. Their accuracies range from around 77% to over 97%, and the average accuracy over the entire set is 92.5%. Almost 60% of the decomposed MUAPTs exhibit accuracy greater than 90%, while fewer than 5% of the decomposed MUAPTs exhibit less than 85% accuracy. The graph in Fig. 9(B) shows that roughly the same split (i.e., 60% of MUAPTs above 90% accuracy and 10% of MUAPTs below 85% accuracy) is found in the decompositions of the 22 reconstructed signals.

We wish to emphasize that the average accuracy value obtained through the reconstruct-and-test procedure represents the accuracy throughout a very large number of 561 MUAPTs, including all the MUAPTs identified in 22 contractions in five different muscles. All the firings of the motor units are included in the calculation of the accuracy, including the force-increasing and the force-decreasing part of the force profile. It is evident that by choosing selected MUAPTs, or selected segments of the MUAPTs, the average accuracy value would increase. We chose not to provide such selected calculations, but instead to present a measure that represents the real expectation a user of our technology can anticipate when studying the firing behavior of motor units during constant-force and force-varying conditions.

3.6. Accuracy validation

To further validate the accuracy of our sEMG signal decomposition algorithm, we have performed two-source tests of the type first introduced by Mambrito and De Luca (1984). The basic idea behind such tests is to carry out cross-checking of the independent decompositions of the signals obtained from different sensors for the same muscle contraction. In De Luca et al. (2006), the decomposition (using an earlier version of our technique) of the signal from a surface sensor was compared to the decomposition of the signal from a co-located indwelling sensor. To make the validation test even more challenging this time, we performed the two-source test on pairs of sEMG signals that were simultaneously acquired from two closely spaced sEMG sensors. For example, when we placed two sEMG sensors above an FDI muscle performing an isometric contraction that reached 50% MVC, the two signals were decomposed by our algorithm to reveal 30 and 31 MUAPTs, respectively. Upon analysis of these decomposition results, we found that over 92% of 3456 firings of 11 of the decomposed MUAPTs of the signal from one sensor were locked in with the firings of 11 corresponding MUAPTs decomposed from the other sensor's signal. The highest lock-in rate of any of the 11 locked-in MUAPT pairs was 98% while the lowest lock-in rate of any of them was 87%. This measure of accuracy provides nearly identical results to that obtained with the above described synthesize-and-test procedure. In Fig. 10(A), we show the bar plots of the 11 MUAPTs of each of the two sensor signals. The magnified interval of 2 s in Fig. 10(B) from the two bar plots in Fig. 10(A) illustrates the locked-in behavior exhibited by matching pairs of decomposed

MUAPTs of the two sensor signals. One error occurred near the 13 s mark. Finally, we also note that there was perfect agreement between the decompositions of the two sensor signals about the recruitment order of the 11 common motor units, a strong indication that our algorithm effectively captures the recruitment order of the various motor units.

Although compelling, the results of the “two sensor” procedure provide a less rigorous and a less complete test than the above described “reconstruct-and-test” procedure. The two sensor test can only compare the accuracy of the MUAPTs that are common to the signals from each of the sensors. The accuracy of the remainder of the MUAPTs is not known. Whereas, the reconstruct and test procedure measures the accuracy of all the MUAPTs that are decomposed.

3.7. Data-driven behavior

The reported algorithm's behavior is data-driven in three important respects. First, if the algorithm is applied at different times to identical input signals, it produces identical output data each time. Second, if the input data of the algorithm is multiplied by a fixed non-zero constant, the output data of the algorithm remains unchanged except for the scaling of the estimated action potential shapes by the same fixed constant. Third, the algorithm's operation is based solely on the assumption that the input sEMG signal originates from an isometric contraction of a human muscle. It does not utilize any other inputs such as information identifying the muscle or the force profile of the contraction.

3.8. Processing speed versus accuracy

As indicated in Table 1, the algorithm takes on the order of 3–4 s to obtain 1 s of each decomposed MUAPT when executed on a state-of-the-art Personal Computer. This is 3–4 times slower than our most accurate decomposition algorithm for indwelling EMG signals (Nawab et al., 2008). However, it is possible to speed up the algorithm significantly by sacrificing accuracy. For example, we have speeded up the algorithm by a factor of 3–4 but the resulting accuracy is typically around 80% for the same number of decomposed MUAPT constituents as found by the most accurate version of the algorithm.

4. Discussion

The algorithm described in this report was able to automatically decompose sEMG signals collected from various muscles contracting isometrically at force levels ranging up to 100% MVC. We were able to decompose sEMG signals from locations where the muscle was covered with up to 1.5 cm of adipose tissue. The number of MUAPTs obtained from the contractions varied among muscles and force levels. It ranged from 20 to 30 MUAPTs, with a present maximum of 40 obtained from a 75% MVC in the Biceps Brachialis muscle. See Table 1 for additional details. The accuracy of the firing times of each of the identified MUAPTs was on average 92.5%, and in rare cases reaching levels above 97%. This performance is achieved for all signals that are collected on a clean skin surface, with the sensor firmly attached to the skin, and without any clipping in the sEMG signal.

The reported system's decomposition performance at a variety of force levels (up to 100% MVC) stands in contrast to that of recently reported sEMG signal decomposition systems that use a convolutional blind signal separation (CBSS) approach (Holobar and Zazula, 2007; Holobar et al., 2009) in conjunction with high-density sEMG sensors. The CBSS approach does not use template matching during decomposition and has been reported to succeed in decomposing

⁶ Following Nawab et al. (2008), the decomposition accuracy (A) for a MUAPT is determined from the number of firings (N_{FIR}), the number of false positives (N_{FP}), and the number of false negatives (N_{FN}) in the decomposition: $A = \frac{N_{\text{FIR}} - N_{\text{FP}} - N_{\text{FN}}}{N_{\text{FIR}}} \times 100\%$.

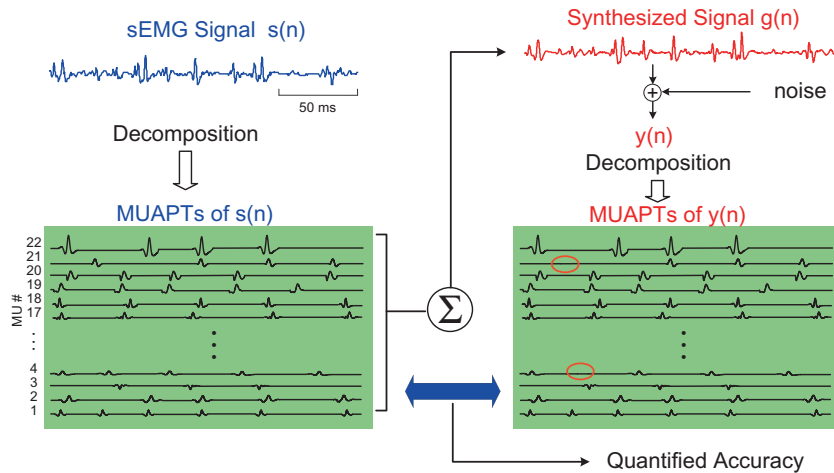


Fig. 8. Illustration of “reconstruct-and-test” procedure for assessing the accuracy of the decomposition algorithm. An actual sEMG signal $s(n)$ is decomposed to identify its MUAPTs. Signal $y(n)$ is synthesized by summing together the decomposed MUAPTs of $s(n)$ and white Gaussian noise whose variance is set equal to that of the residual signal from the decomposition. The reconstituted $y(n)$ signal is then decomposed and compared to the decomposed MUAPTs of $s(n)$. The ellipses indicate discrepancies between the MUAPTs of $y(n)$ and $s(n)$. These are designated as errors.

sEMG signals collected from isometric contractions whose force levels rise slowly to a level less than 10% MVC and then are slowly decreased. Low-force contractions of this type ensure that the number of active motor units at any time during the contraction is low enough to avoid high degrees of superposition. Furthermore, they help to mitigate decomposition errors that result from the fact that the sEMG signal violates some of the foundational mathematical assumptions underlying the CBSS approach:

CBSS models the input sEMG signal as consisting of decomposable MUAPTs that are in turn summed with spatially and temporally independent samples of “noise” (Holobar and Zazula, 2007). However, the “noise” in the real sEMG signal is dominated by the contributions of indecomposable MUAPTs (De Luca et al., 2006). Given that the high-density sEMG sensor is designed to ensure that the set of MUAPTs detected at each of its numerous electrodes remains essentially invariant, the “noise” component of the sEMG signal does not meet the criterion of spatial and temporal independence.

CBSS assumes (Holobar and Zazula, 2007) “weakly correlated” firing times of MUAPTs. This runs afoul of physiological reality because of phenomena such as the common drive (De Luca et al., 1982; De Luca and Erim, 1994; McGill et al., 2005, among others) of different motor units.

CBSS assumes (Holobar and Zazula, 2007; Holobar et al., 2009) that the shape of the action potential of a motor unit remains constant throughout a contraction, even though that is not borne out in actual sEMG signals. For example, in Fig. 11(A) we show how the shape of the action potential of a particular MUAPT is found to change by the algorithm of this report at 1 s, 11 s, and 21 s into the constant-force region of a trapezoidal contraction of the FDI muscle at 50% MVC.

In contrast to CBSS, our template-matching approach, enhanced by artificial intelligence methods, avoids each of the above mathematically imposed restrictions. More specifically:

- With respect to the indecomposable MUAPTs, our approach treats their signal contributions as being composed of action potentials whose shapes are not accurately determinable from the signal because of either their low amplitudes or their high rates of superposition with the action potentials of other MUAPTs. Thus, there is no constraint placed on their signal contributions to be spatially or temporally independent.

- In regard to correlations of the firing times of different MUAPTs, our approach does explicitly exclude the possibility of any pair of decomposable MUAPTs having more than 10 instances (within any 30 s interval) where they have identical firing times while also not being involved in superposition with any of the other MUAPTs. There are, however, no further constraints imposed on how the firing times of different MUAPTs may or may not be correlated.
- As to the issue of allowing changes in the action potential shape, our approach explicitly allows the action potential shape of each MUAPT to evolve over the duration of a contraction, as was incorporated into the original Maximum A-posteriori Probability (MAP) classifier of Lefever and De Luca (1982).

The five muscles used for the tests were chosen to represent different challenges to the algorithm. The FDI was chosen because it is a small muscle containing about 120 motor units (Feinstein et al., 1955) in a relatively small volume and the muscle is covered by a thick loose skin. The remaining muscles have a greater number of motor units, ranging up to approximately 774 in the BB (Buchthal, 1961). The TA and the BB muscles are large muscles that usually have little adipose tissue between the muscle tissue and the relatively thin skin above them. The VL and the BF are relatively large muscle commonly having up to 1 cm of adipose tissue between the surface of the muscle and the skin in most non-obese subjects, and more in obese subjects. The sEMG signal from the BF presented a serious challenge to the decomposition algorithm due to the 1.5 cm of adipose tissue in the subjects who contributed the sample contractions in the database.

The ultimate goal of any algorithm for decomposing the sEMG signal is to provide accurate and physiologically meaningful data about the underlying MUAPT activity. Achievement of this objective is made difficult by: (1) the occurrence of excessive amounts of superposition between the action potentials of different MUAPT constituents of the sEMG signal; (2) subtle changes in shape of the different action potentials contained in each MUAPT; and (3) high degree of inter-MUAPT similarity of action potential shapes. The challenge of these factors to sEMG signal decomposition is proportionately greater when the tissue above the muscle is excessive causing a decrease in the amplitude of the signal, or when the number of MUAPT constituents

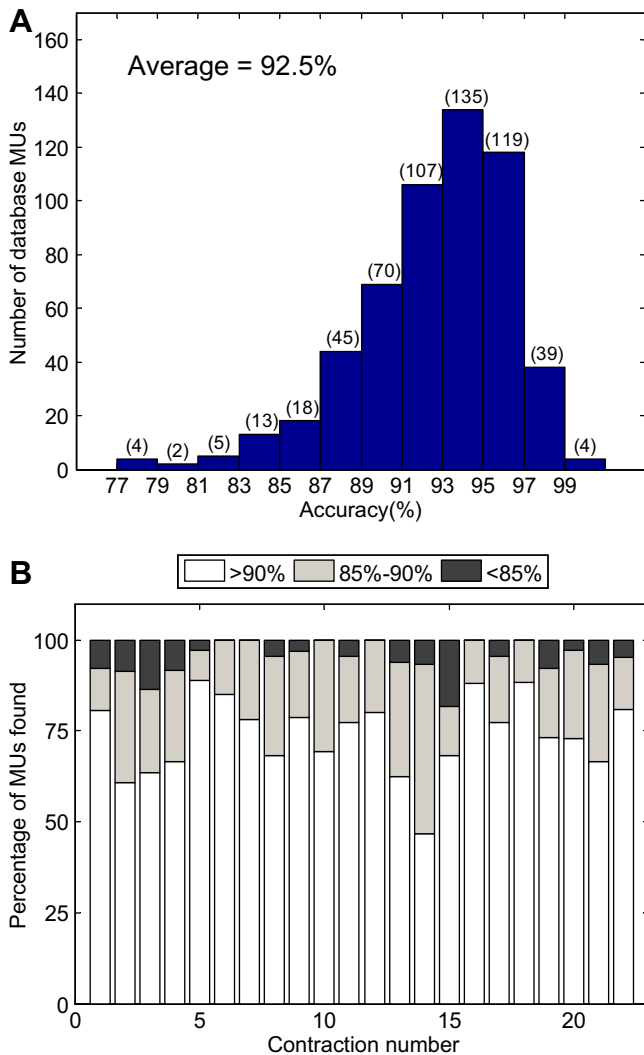


Fig. 9. (A) Histogram plot indicating the accuracies (expressed as percentages) of the decomposition for the 561 MUAPTs of the entire set of sEMG signals listed in Table 1. The mean \pm standard deviation of the accuracies is 92.5 ± 3.7 percent. (B) Bar graph of the MUAPT accuracy distribution for each of the 22 signals listed in Table 1. The non-shaded portion of each signal's bar indicates the percentage of its MUAPTs that have accuracy above 90%. The gray portion of each bar indicates the percentage of a signal's MUAPTs that have accuracies between 85% and 90%. The darkest portion of each bar represents the percentage of a signal's MUAPTs with accuracies below 85%.

and/or their firing rates increase, as happens when a muscle generates a greater force.

4.1. Shape changes

The changes in action potential shape of a MUAPT are much more subtle in the sEMG signal when compared to those found in the indwelling EMG signal (Nawab et al., 2008). Nevertheless, we have found it useful to track the dynamics of shape change in each decomposed MUAPT of the sEMG signal in order to avoid some of the identification errors that arise when two MUAPT constituents have similarly-shaped action potentials. As illustrated in Fig. 11(A), the energy of an action potential of a particular MUAPT can vary by an amount on the order of 5%. Farina et al. (2008) have also pointed out the existence of such variations. It is precisely because of such variations that our Precision Decomposition approach since the earliest work of LeFever and De Luca (1982) has

always incorporated mechanisms for tracking the dynamics of shape change within each action potential train to distinguish it from other trains of similarly-shaped action potentials.

4.2. Shape similarity

In comparison to the case of indwelling EMG signals, a MUAPT of the sEMG signal has a much greater likelihood of its action potential shape being similar to that of another MUAPT constituent. Shape similarity of action potentials is illustrated in Fig. 11(B) for three different MUAPTs of the sEMG signal acquired from a BB muscle at 50% MVC. The algorithm was able to identify each shape as belonging to a different MUAPT even though the differences between the action potential shapes in Fig. 11(B) are of the same order as the differences between the action potential shapes in Fig. 11(A) for a single MUAPT. It should be noted that in order to identify similarly-shaped action potentials as belonging to different MUAPTs, our algorithm explicitly rules out the possibility that they belong to the same underlying MUAPT. It does so by (1) finding instances where the different action potential shapes are in superposition with each other and by (2) verifying that the combined firings of the two MUAPTs would produce too many instances of unreasonably small inter-pulse intervals.

4.3. Excessive superposition

The challenge of excessive MUAPT superposition in sEMG signals is illustrated by the top plot in Fig. 12 that shows one channel of a filtered 20 ms segment of the sEMG signal obtained from the FDI muscle at 50% MVC. The reported algorithm reveals this segment to be the superposition of nine different action potentials, as shown in the remaining plots of Fig. 12. This result was also verified by the accuracy evaluation test that is described in Section 3. Note that while some of the MUAPT constituents of the segment are readily apparent to the naked eye, others are essentially buried under larger action potentials. In cases such as this, the algorithm makes two types of errors; an "identification error" or a "positioning error". An identification error is one in which the action potential of one MUAPT is mistaken for a similarly-shaped action potential of another MUAPT. A positioning error is one whereby an action potential cannot be located precisely. Even if a MUAPT is correctly identified, the relative smoothness of the shapes of the constituent action potentials in Fig. 12 makes it likely for a positioning error to occur. The likelihood of a positioning error is greater for low amplitude motor units because (1) they have shallower peaks whose maxima are difficult to identify precisely and (2) they have greater chance of being "buried" via superposition with larger action potentials. It is for this reason that at the end of our algorithm each firing of a decomposed MUAPT of relatively low amplitude is slightly re-positioned by cross-correlating its action potential template with a modified version of the sEMG signal in the vicinity of the firing. Specifically, the modification to the sEMG signal involves subtracting off the action potential templates of higher-amplitude MUAPTs that are at least partially superimposed with the firing under consideration.

4.4. Dynamic range of MUAPT amplitudes

As illustrated by the action potential plots in Fig. 7, the lowest-amplitude MUAPTs decomposed by our algorithm tend to be several times smaller than the MUAPT with the largest amplitude. It follows that the lower amplitude motor units have a tendency to get "buried" whenever they are superimposed to a significant extent by the larger amplitude MUAPTs. This might lead one to suspect that the lower-amplitude MUAPTs are generally decomposed

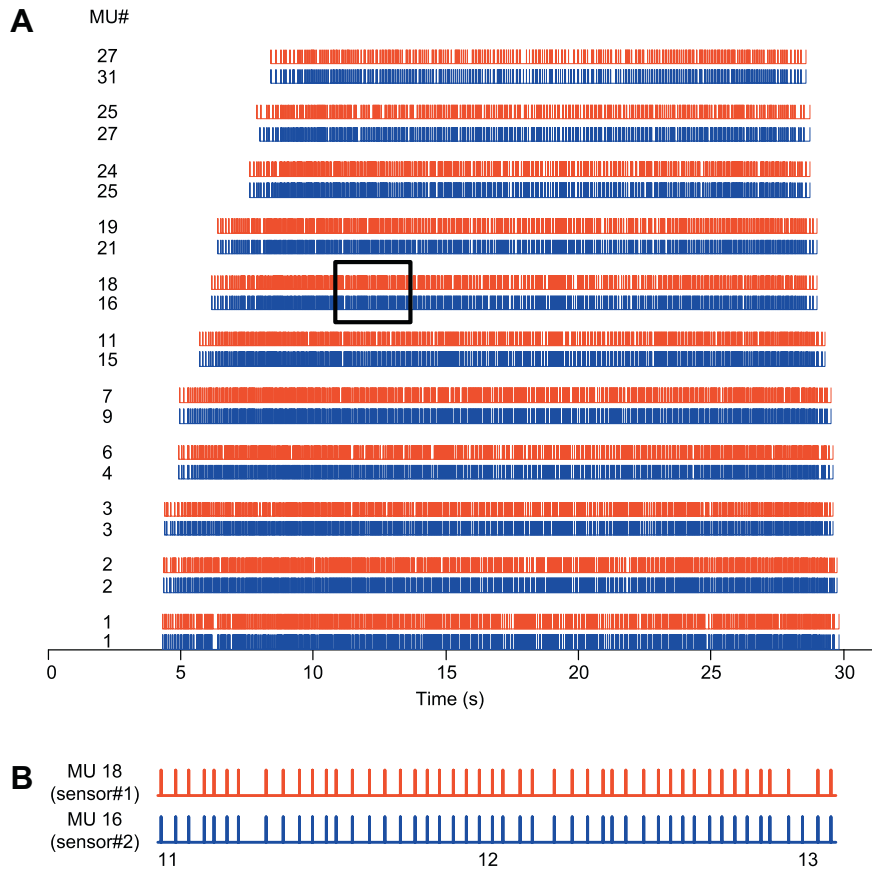


Fig. 10. (A) A comparison of all the firings of 11 MUAPTs that were identified by the decomposition of two signal sets obtained from two sensors located on the First Dorsal Interosseous muscle contracting at 50% MVC. The first signal set decomposed into 30 MUAPTs and the second into 31 MUAPTs. Eleven (11) were common in both signals sets. The blue bars correspond to the MUAPTs from sensor #1 while the black bars correspond to those of sensor #2. (B) A magnified interval of 2 s from the two bar plots illustrates the simultaneous occurrence of the firings from an individual motor unit seen in each of the two sensors.

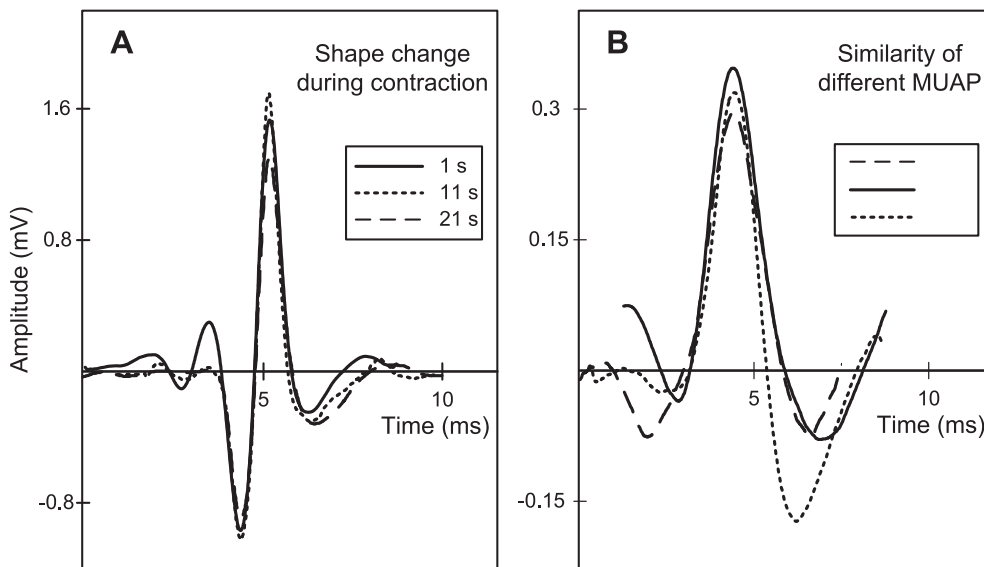


Fig. 11. (A) An illustration of changing MUAP shapes of a motor unit throughout a contraction. The three shapes represent the MUAP of the same motor unit as it appears at different times (1, 11, and 21 s) in the steady region of a contraction. (B) An illustration of the similarity of the shapes of different MUAPs occurring during an epoch of a contraction.

less accurately by our algorithm than their larger amplitude counterparts. This turns out not to be the case. Instead, the accuracy of decomposition of the lower-amplitude MUAPTs is helped

by two factors. First, each lower-amplitude MUAPT typically has a relatively greater firing rate than its higher amplitude counterparts and thus tends to provide our algorithm more instances of

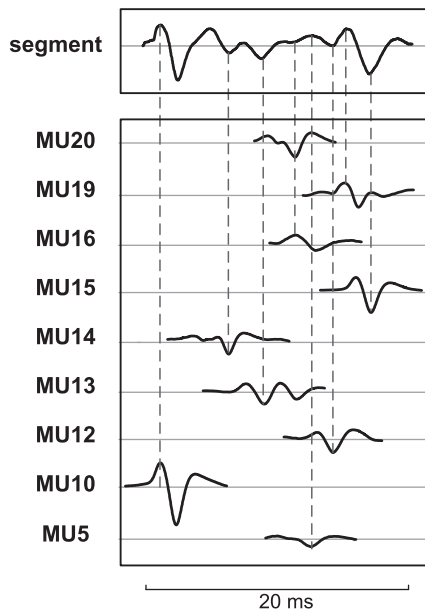


Fig. 12. Top Plot: A single channel of a filtered 12 ms segment of the sEMG signal obtained from the First Dorsal Interosseous muscle contracting at 50% MVC. Bottom Plots: Nine motor unit action potentials found by the sEMG decomposition algorithm to be in superposition in the 20 ms segment. The sum of all 9 Motor unit action potentials yields the trace in the top plot. This figure shows the capacity of the decomposition algorithm to extract action potentials from a complex superposition.

firings that are not contaminated by superposition. Furthermore, the low-amplitude firings contaminated by superposition are aided by a “re-positioning” process in which higher-amplitude MUAPs are peeled off from the sEMG signal to more precisely position the lower-amplitude MUAPs. Of course, these two factors help only up to a certain point. MUAPs whose amplitudes are too low (typically 7–10 times smaller than the largest amplitude MUAP) are typically ignored by our current version of the algorithm because their shapes are too “flat” or non-descript to be easily distinguished from each other or to be detected with sufficient confidence amidst superposition by larger amplitude MUAPs.

4.5. Compatibility with previous physiological metrics

The firing characteristics of motor units obtained by the present algorithm have values that are consistent with those obtained with our previous algorithms operating on indwelling EMG signals, and with the reported observations of others. A summary of the findings are reported here. When we calculated the degree of synchronization of firings between pairs of motor units according to the method of De Luca et al. (1993), we found the value to range from 4% to 15%. These values are consistent with those obtained with indwelling EMG signal decomposition (De Luca et al., 1993) and with those of Semmler and Nordstrom (1998) and Semmler et al. (2000) who also decomposed indwelling EMG signals. We also tested the coefficient of variation of the inter-pulse intervals and found values in the neighborhood of 0.10–0.15, numbers that are consistent with those reported by Moritz et al. (2005) and Tracy et al. (2005). The near maximal firing rates of the FDI were found to reach values of 37 pulses per second, whereas those of larger muscles such as the VL only reached lower values. These values are in agreement with previous reports by De Luca et al. (1982), Gandevia et al. (1990), Erim et al. (1999), Roos et al. (1999), Adam and De Luca (2005), and Seki et al. (2007). These tests support the notion that the motor

unit firing intervals automatically obtained with the present algorithm are consistent with known physiological characteristics of the firing behavior of motor units.

4.6. Potential clinical applications

The design of the pin lay-out in the sensors renders the sensor easy to clean. The small size of the sensor makes it useful for investigating the motor unit behavior of small muscles such as those in the hand and face. The requirement of only few (presently four) channels of sEMG signals constrains the electronics of the system to a small, manageable unit.

The technology described herein has the potential of providing clinicians with a new tool for investigating and assessing the characteristics of active motor units. It can provide all the information presently provided by invasive needle sensor techniques as well as additional parameters which are generally not presently used in clinical studies.

Like the needle technology used in clinical environments, our technology can also provide information about the morphology of the action potentials. But unlike present needle technology, it is not limited to the short-term viewing of action potentials from two or three motor units. Our technology typically presents the morphology of the shapes of up to 40 concurrently active motor units, without relocating the sensor. It also provides an entire spectrum of motor units that allows investigators to analyze higher threshold motor units. For example, Fig. 13 presents polyphasic MUAPs seen in elderly individuals. These data were obtained from tests, similar to those described in Section 2, performed on elderly subjects. There are two interesting aspects to these data. Firstly, it is apparent that polyphasic MUAPs can be detected with our sEMG technology. Secondly, it is possible to obtain polyphasic MUAPs from low-level contractions (10% MVC) as shown in the top part of Fig. 13, as well as from high-level contractions (45% MVC) as shown in bottom part of Fig. 13.

Some of the firing parameters of the motor units that can be extracted from the decomposition of the sEMG signal are:

- The standard deviation and coefficient of variation of the firing intervals which provide an assessment of the degree of firing regularity.
- The recruitment and de-recruitment thresholds of motor units which have been found to vary during fatigue (Adam and De Luca, 2003).
- The time-varying firing rates of the motor units which indicate the degree of excitation to the motoneurons during the time course of a contraction.
- The common drive (the cross-correlation of the time-varying firing rates of pairs of motor units) that provides an assessment of the degree of common excitation to the motoneuron pool. Alterations in this parameter have been found in acute cerebellar patients (Sauvage et al., 2006), in elderly, but neurologically healthy, subjects (Erim et al., 1999), and during fatigue (Contessa et al., 2009).
- The synchronization of firings among motor units, alterations of which have been reported under a variety of circumstances in healthy subjects. But, this parameter which indicates common instantaneous excitation among motoneurons has not yet been explored in clinical studies.

This new information may provide further insights into the pathophysiology of disease processes while providing clinical applications in earlier disease detection, monitoring disease progression and evaluating efficacy of therapeutic interventions, especially for upper motoneuron disorders.

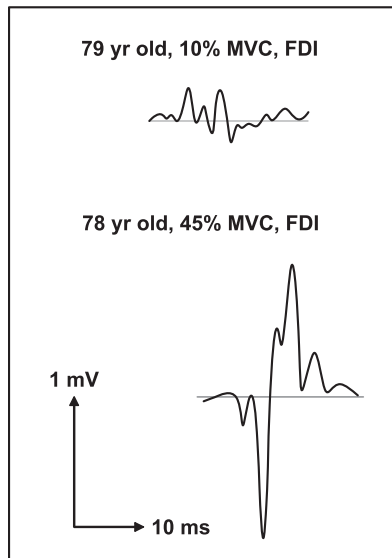


Fig. 13. Polyphasic action potentials derived from the decomposition of surface EMG signals. Both are from elderly subjects, 79 and 78 years old. Both samples were obtained from the First Dorsal Interosseous (FDI) muscle. The polyphasic action potential in the top trace was from a motor unit recruited at 10% MVC and that in the bottom trace from a motor unit recruited at 45% MVC.

Acknowledgements

This work was supported in part by Grant # NS058250 from NINDS/NIH and in part by Delsys Inc. We would like to thank Bryan Cole and Jason Lin for their assistance in algorithm implementation and Prof. Serge Roy, Don Gilmore, Farah Zaheer, Jeff Soto, Paola Contessa, Emily Hostage, and Mikhail Kuznetsov for their assistance in data collection and analysis.

References

- Aarabi A, Grebe R, Wallois F. A multistage knowledge-based system for EEG seizure detection in newborn infants. *Clin Neurophysiol* 2007;118:2781–97.
- Adam A, De Luca CJ. Recruitment order of motor units in human vastus lateralis muscle is maintained during fatiguing contractions. *J Neurophysiol* 2003;90:2919–27.
- Adam A, De Luca CJ. Firing rates of motor units in human vastus lateralis muscle during fatiguing isometric contractions. *J Appl Physiol* 2005;99:268–80.
- Bárdossy A, Samaniego-Eguiguren LE. Fuzzy rule-based classification of remotely sensed imagery. *IEEE Trans Geosci Remote Sens* 2002;40:362–74.
- Buchthal F. The general concept of the motor unit neuromuscular disorders. *Res Publ Assoc Res Nerv Ment Dis* 1961;38:3–30.
- Chang S, De Luca CJ, Nawab SH. Aliasing rejection in precision decomposition of EMG signals. In: 30th annual international conference of the IEEE engineering in medicine and biology society, Vancouver, Canada, 2008, pp. 4972–75.
- Contessa P, Adam A, De Luca CJ. Motor unit control and force fluctuation during fatigue. *J Appl Physiol* 2009;107:235–43.
- De Luca CJ, Adam A. Precision decomposition of intramuscular electromyographic signals. In: Windhorst U, Johansson H (Eds), *Modern techniques on neuroscience research*. Heidelberg: Springer; 1999. pp. 757–76.
- De Luca CJ, Adam A, Wotiz RP, Gilmore LD, Nawab SH. Decomposition of surface EMG signals. *J Neurophysiol* 2006;96:2769–74.
- De Luca CJ, Erim Z. Common drive of motor units in regulation of force. *Trends Neurosci* 1994;17:299–305.
- De Luca CJ, Erim Z. Common drive in motor units of a synergistic muscle pair. *J Neurophysiol* 2002;87:2200–4.
- De Luca CJ, Foley PJ, Erim Z. Motor unit control properties in voluntary isometric isotonic contractions. *J Neurophysiol* 1996;76:1503–16.
- De Luca CJ, Roy AM, Erim Z. Synchronization of motor unit firings in human muscles. *J Neurophysiol* 1993;70:2010–23.
- De Luca CJ, LeFever RS, McCue MP, Xenakis AP. Behavior of human motor units in different muscles during linearly-varying contractions. *J Physiol* 1982;329:113–28.
- Englehart K, Hudgins B, Parker PA, Stevenson M. Classification of the myoelectric signal using time-frequency based representations. *Med Eng Phys* 1999;21:431–8. Special issue: intelligent data analysis in electromyography and electroneurography.
- Englehart K, Hudgins B, Parker PA. A wavelet based continuous classification scheme for multifunction myoelectric control. *IEEE Trans Biomed Eng* 2001;48:302–11.
- Erim Z, Beg MF, Burke DT, De Luca CJ. Effects of aging on motor-unit control properties. *J Neurophysiol* 1999;82:2081–91.
- Erim Z, Lin W. Decomposition of intramuscular EMG signals using a heuristic fuzzy expert system. *IEEE Trans Biomed Eng* 2008;55:2180–9.
- Farina D, Negro F, Gazzoni M, Enoka RM. Detecting the unique representation of motor-unit action potentials in the surface electromyogram. *J Neurophysiol* 2008;100:1223–33.
- Feinstein B, Lindgard B, Nyman E, Wohlfart G. Morphological studies of motor units in normal human muscles. *Acta Anat* 1955;23:127–42.
- Gandevia SC, Macefield G, Burke D, McKenzie DK. Voluntary activation of human motor axons in the absence of muscle afferent feedback, the control of the deafferented hand. *Brain* 1990;113:1563–81.
- Gini F, Rangaswamy M. Knowledge based radar detection, tracking and classification. Wiley-Interscience; 2008.
- Holobar A, Zazula D. Multichannel blind source separation using convolution kernel compensation. *IEEE Trans Signal Process* 2007;55:4487–96.
- Holobar A, Farina D, Gazzoni M, Merletti R, Zazula D. Estimating motor unit discharge patterns from high density surface electromyogram. *Clin Neurophysiol* 2009;120:551–62.
- Jiang N, Englehart KB, Parker PA. Extracting simultaneous and proportional neural control information for multiple-DOF prostheses from the surface electromyographic signal. *IEEE Trans Biomed Eng* 2009;56:1070–80.
- Kundu M, Nasipuri M, Kumar Basu D. Knowledge-based ECG interpretation: a critical review. *Pattern Recogn* 2000;33:351–73.
- Leake D. Case-based reasoning: experiences, lessons, and future directions. AAAI Press/MIT Press; 2000.
- LeFever RS, De Luca CJ. A procedure for decomposing the myoelectric signal into its constituent action potentials. Part I. Technique, theory and implementation. *IEEE Trans Biomed Eng* 1982;29:149–57.
- Leondes CT. Knowledge-based systems: techniques and applications. Academic Press; 2000.
- Lesser V, Nawab SH, Klassner F. IPUS: an architecture for the integrated processing and understanding of signals. *Artif Intell* 1995;77:129–71.
- Ligeza A. Logical foundations for rule-based systems. Springer; 2006.
- Mambrito B, De Luca CJ. A technique for the detection, decomposition and analysis of the EMG signal. *Electroencephal Clin Neurophysiol* 1984;58:175–88.
- McGill KC, Lateva ZC, Marateb HR. EMGLAB: an interactive EMG decomposition program. *J Neurosci Methods* 2005;149:121–33.
- Merletti R, Parker PA. Electromyography: physiology, engineering, and non-invasive applications. IEEE press series on biomedical engineering. Wiley-IEEE Press; 2004.
- Moritz CT, Barry BK, Pascoe MA, Enoka RM. Discharge rate variability influences the variation in force fluctuations across the working range of a hand muscle. *J Neurophysiol* 2005;93:2449–59.
- Nawab SH, Chang S, De Luca CJ. Surface EMG signal decomposition using empirically sustainable biosignal separation principles. In: Proceedings of the thirty-first international conference of the IEEE engineering in medicine and biology society, Minneapolis, Sept. 2–6, 2009.
- Nawab SH, Wotiz R, De Luca CJ. Decomposition of Indwelling EMG Signals. *J Appl Physiol* 2008;105:700–10.
- Nawab SH, Wotiz RP, De Luca CJ. Multi-Receiver precision decomposition of indwelling EMG signals. In: Proceedings of the twenty-eighth international conference of the IEEE engineering in medicine and biology society, New York City, 2006, pp. 1252–55.
- Nawab SH, Wotiz RP, De Luca CJ. Improved resolution of pulse superpositions in a knowledge-based system for EMG decomposition. In: Proceedings of the twenty-sixth international conference of the IEEE engineering in medicine and biology society, San Francisco, CA, September 2004, pp. 69–71.
- Nawab SH, Wotiz RP, Hochstein LM, De Luca CJ. Next-generation decomposition of multi-channel EMG signals. In: Proceeding of the 2nd joint meeting IEEE engineering in medicine and biology society and biomedical engineering society, Houston, TX, October 2002, pp. 36–7.
- Person RS. Rhythmic activity of a group of human motoneurons during voluntary contraction of a muscle. *Electroencephalogr Clin Neurophysiol* 1974;36:585–95.
- Roos MR, Rice CL, Connelly DM, Vandervoort AA. Quadriceps muscle strength, contractile properties, and motor unit firing rates in young and old men. *Muscle Nerve* 1999;22:1094–103.
- Sauvage C, Manto M, Adam A, Roark R, Jissendi P, De Luca CJ. Ordered motor unit firing behavior in acute cerebellar stroke. *J Neurophysiol* 2006;96:2769–74.
- Seki K, Kizuka T, Yamada H. Reduction in maximal firing rate of motoneurons after 1-week immobilization of finger muscle in human subjects. *J Electromyogr Kinesiol* 2007;17:113–20.
- Semmler JG, Nordstrom MA. Motor unit discharge and force tremor in skill- and strength-trained individuals. *Exp Brain Res* 1998;119:27–38.
- Semmler JG, Steege JW, Kornatz KW, Enoka RM. Motor-unit synchronization is not responsible for larger motor-unit forces in old adults. *J Neurophysiol* 2000;84:358–66.
- Stashuk DW. Decomposition and quantitative analysis of clinical electromyographic signals. *Med Eng Phys* 1999;21:389–404.
- Stashuk DW. EMG signal decomposition: how can it be accomplished and used? *J Electromyogr Kinesiol* 2001;11:151–73.
- Tanji J, Kato M. Firing rate of individual motor units in voluntary contraction of abductor digiti minimi muscle in man. *Exp Neurol* 1973;40(3):771–83.

- Tracy BL, Maluf KS, Stephenson JL, Hunter SK, Enoka RM. Variability of motor unit discharge and force fluctuations across a range of muscle forces in older adults. *Muscle Nerve* 2005;32:533–40.
- Winograd JM, Nawab SH. A C++ software environment for the development of embedded signal processing systems. In: Proceedings of IEEE international conference on acoustics, speech, and signal processing, Detroit, MI, 1995, pp. 2715–18.
- Zhou P, Lowery MM, Rymer WZ. Extracting motor unit firing information by independent component analysis of surface electromyogram: a preliminary study using a simulation approach. *Int J Comp Syst Signals* 2006;7:19–28.